Matter

CellPress

Article

Continuous lithium extraction from brine by efficient redox-couple electrodialysis

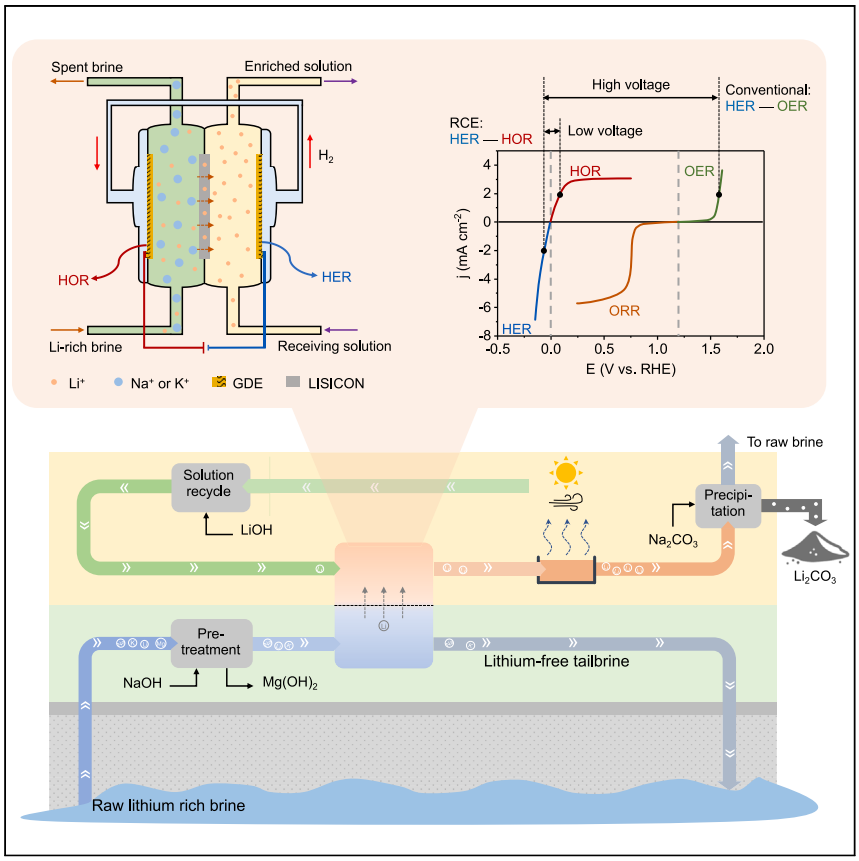

Can we replace the inefficient, costly, and environmentally harmful traditional methods of Li mining with a sustainable and economical process? The authors present an efficient redox-couple electrodialysis (RCE) method for sustainable Li extraction from salt-lake brines. The benefits to efficiency and cost innate to their RCE approach make it a promising alternative to current extraction techniques and a potential game changer for the Li supply chain.

Rong Xu, Xin Xiao, Ge Zhang, ..., Yufei Yang, Sanzeeda Baig Shuchi, Yi Cui

yicui@stanford.edu

Highlights

An efficient redox-couple electrodialysis to realize sustainable Li extraction

Zero-equilibrium voltage and low overpotential for redox-couple electrodialysis

Li extraction with an ultralow voltage, a high efficiency, and a high selectivity

A substantially reduced cost compared to conventional Li extraction routes

6 **Development**
Practical, real world, technological considerations and constraints

Xu et al., Matter 7, 1–15
November 6, 2024
https://doi.org/10.1016/j.matt.2024.07.014

Please cite this article in press as: Xu et al., Continuous lithium extraction from brine by efficient redox-couple electrodialysis, Matter (2024), https://doi.org/10.1016/j.matt.2024.07.014

Matter

CellPress

Article

Continuous lithium extraction from brine by efficient redox-couple electrodialysis

Rong Xu,[1,5] Xin Xiao,[1,5] Ge Zhang,[1,5] Yusheng Ye,[1] Pu Zhang,[1] Yufei Yang,[1] Sanzeeda Baig Shuchi,[2] and Yi Cui[1,3,4,6,*]

SUMMARY

The rapid growth of lithium (Li)-ion batteries has catalyzed an unprecedented demand for Li. However, global Li supplies struggle to meet the ever-increasing demand because traditional Li mining processes are slow, expensive, and environmentally unsustainable. Here, we introduce an efficient redox-couple electrodialysis (RCE) approach for sustainable Li extraction from brine. The electrodialysis is driven by the same half-cell electrochemical reaction but operated in opposite directions—hydrogen evolution reaction and hydrogen oxidation reaction—which consumes minimal energy due to the zero-equilibrium full-cell voltage and the low overpotential. We demonstrate continuous Li extraction from brine for over 100 h, with a low operating voltage of 0.25 V, a faradaic efficiency of 88.87%, and a Li selectivity of 0.9954. Notably, the Li extraction via RCE consumes the specific energy of a mere 1.1 kWh kg_{Li}^{-1}, an order of magnitude lower than the energy demands of previously reported Li extraction techniques.

INTRODUCTION

The global transition toward renewable energy and transportation electrification has ushered in an unprecedented demand for lithium (Li). Predictions suggest a remarkable escalation, with the need for Li rising from approximately half a million metric tons of Li carbonate equivalent (LCE) in 2021 to an estimated 3–4 million metric tons by 2030.[1] Historically, the primary sources of Li supplies have been terrestrial resources, predominantly mined through salt-lake brines and high-grade ores via evaporation and chemical precipitation techniques. However, these traditional extraction methodologies present multifaceted challenges.[2] Primarily, the adaptability of these methods is limited due to their sensitivity to the unique geological structures of deposits and their dependence on specific climatic and weather conditions.[3] Such limitations not only complicate the establishment of new mining facilities but also substantially inflate capital investments, driving up the costs of resultant Li products. The environmental ramifications of these traditional techniques are also concerning.[4] The extensive chemical processes involved are slow and environmentally detrimental and thus at odds with the push toward a greener and more sustainable society that electrified technologies promise.

In the face of these challenges, direct Li extraction (DLE) techniques, especially those rooted in electrochemical processes such as ion pumping, electrodialysis, and electrolysis, are emerging as viable contenders for Li mining due to their environmental compatibility, high efficiency, procedural simplicity, and adaptability to renewable energy.[5,6] For example, by leveraging the classic intercalation chemistry used in

PROGRESS AND POTENTIAL

Traditional lithium (Li) mining processes are slow, expensive, and environmentally unsustainable. Direct Li extraction (DLE) techniques based on electrodialysis systems have emerged as promising alternatives to conventional approaches, enabling continuous Li extraction from brine and seawater. Here, we introduce a highly efficient redox-couple electrodialysis (RCE) approach to realize sustainable Li extraction from brine with an ultralow operating voltage, a high faradaic efficiency, and a high Li selectivity. Techno-economic analysis reveals that Li extraction via RCE offers a substantially reduced cost compared with traditional Li extraction techniques. The advantages displayed by our RCE approach over conventional Li extraction techniques enhance its feasibility in eco-friendly and cost-effective Li production and could broadly impact the industries of electrified transportation and renewable energy storage.

Please cite this article in press as: Xu et al., Continuous lithium extraction from brine by efficient redox-couple electrodialysis, Matter (2024), https://doi.org/10.1016/j.matt.2024.07.014

rechargeable Li batteries, ion pumping provides an effective strategy for separating Li ions from other competing ions. Many cathode materials for Li-ion batteries, such as $LiFePO_4$ and $LiMn_2O_4$, inherently prefer to incorporate Li over other ions due to the enhanced structural stability of the intercalation products, which boosts the selectivity of Li extraction from mixed-ion sources like brine and seawater.[7–9] However, the necessary post-extraction processes, such as adsorbent regeneration and Li purification, preclude the continuous operation of ion-pumping systems, introducing substantial efficiency, economic, and environmental costs.[10]

Electrochemical DLE based on electrodialysis or electrolysis systems offers the potential for continuous Li extraction from brine and seawater.[11–13] However, the practical application of this approach seems challenging, partially due to the limited availability of membranes that combine high Li selectivity and ionic conductivity. Recent advancements in solid-state Li battery technology have unveiled a broad spectrum of solid-state electrolytes (SSEs) that exhibit commendable Li conductivity and selectivity.[14] Oxide ceramic electrolytes are particularly important due to their high stability in aqueous solutions. Notable examples include NASICON (sodium super ionic conductor)-type $Li_{1.5}Al_{0.5}Ge_{1.5}(PO4)_3$ (LAGP)[15] or $Li_{1.5}Al_{0.5}Ti_{1.5}(PO4)_3$[16] and perovskite-type $Li_{0.33}La_{0.56}TiO_3$.[17] Several current prototypes that employ SSE as the Li-ion selective membrane have demonstrated significant promise for continuous Li extraction from brine and seawater with high selectivity. However, these prototypes often operate at high voltages due to the substantial redox potential difference between the two electrodes,[6] making the overall process energy intensive. Additionally, they experience diminished faradaic efficiency due to side reactions at both electrodes.[11] These inefficiencies raise the operational cost of DLE, thereby inflating the end-product price. Photoelectrochemical[18,19] and photothermal[20] effects have been integrated into electrodialysis systems to enable green and sustainable Li extraction, but the expensive materials and delicate structures hinder the scale-up of these devices. Consequently, there is a pressing need for a practical design that facilitates continuous Li extraction while ensuring low operational voltages and maintaining high faradaic efficiency, all in the pursuit of sustainable Li mining.

Here, we introduce a highly efficient redox-couple electrodialysis (RCE) approach to realize sustainable Li extraction from salt-lake and oil-extraction brines. The same half-redox reaction is used here as the driving force for electrodialysis but operated in the opposite direction: hydrogen evolution reaction (HER) and the hydrogen oxidation reaction (HOR). The same half-reaction offers the zero equilibrium full cell voltage, and HER/HOR has proven to have very low overpotential under realistic current density.[21] Furthermore, the introduction of a Li-ion selective SSE membrane ensures that only Li ions can transport through the membrane from the brine to the receiving solution, leading to high selectivity and faradaic efficiency for Li extraction. The working mechanism of Li extraction via RCE is depicted in Figure 1A. In the right chamber, a LiOH solution flows in, where water undergoes reduction to produce OH^- and H_2 at the anode via HER (Equation 1); in the left chamber, Li-rich brine is supplied, and the H_2 produced in the right chamber flows to the left gas chamber and then reacts with the OH^- in the brine to form water at the cathode via HOR (Equation 2).

$$\text{Anode}: 2H_2O + 2e^- \rightarrow H_2\uparrow + 2OH^- \quad \text{(Equation 1)}$$

$$\text{Cathode}: 2H_2 + 2OH^- \rightarrow 2H_2O + 2e^- \quad \text{(Equation 2)}$$

[1]Department of Materials Science and Engineering, Stanford University, Stanford, CA 94305, USA

[2]Department of Chemical Engineering, Stanford University, Stanford, CA 94305, USA

[3]Department of Energy Science and Engineering, Stanford University, Stanford, CA 94305, USA

[4]Stanford Institute for Materials and Energy Sciences, SLAC National Accelerator Laboratory, Menlo Park, CA 94025, USA

[5]These authors contributed equally

[6]Lead contact

*Correspondence: yicui@stanford.edu

https://doi.org/10.1016/j.matt.2024.07.014

Please cite this article in press as: Xu et al., Continuous lithium extraction from brine by efficient redox-couple electrodialysis, Matter (2024), https://doi.org/10.1016/j.matt.2024.07.014

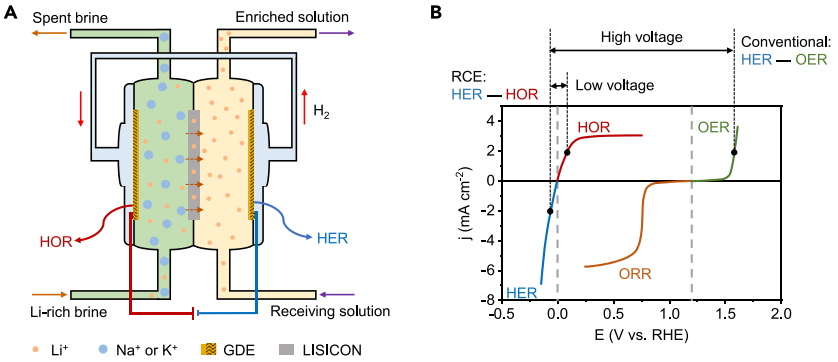

Figure 1. Working mechanism of continuous Li extraction via RCE

(A) Schematic of the flow cell designed for the continuous Li extraction from feeding brine to the receiving solution. LISICON, lithium super-ionic conductor.

(B) A comparison between traditional electrochemical DLE methods and our RCE method. Our design employs the reversible redox pair of HER and HOR, offering an equilibrium potential of zero and a substantially reduced polarization potential with increasing current density.

Driven by the electric field within the electrolyte, Li ions migrate from the left chamber to the right, enriching the LiOH solution therein. A distinguishing feature of our RCE design is its reliance on the reversible redox couple of HER and HOR, with a theoretical equilibrium potential of zero. Meanwhile, as the current density rises for HER or HOR, the polarization potential remains significantly lower than in other reactions, as illustrated in Figure 1B. These unique features of RCE allow Li extraction to operate at an ultralow voltage (~100 mV), offering its advantages in energy and cost efficiency. By contrast, several recent DLE prototypes via electrodialysis are anchored in the oxygen evolution reaction (OER) or the chlorine evolution reaction (CER) paired with HER. They suffer from the high thermodynamic potential difference between OER (or CER) and HER, as well as the large kinetic overpotentials resulting from sluggish reactions, often leading to operational voltages well above 3.0 V.

RESULTS AND DISCUSSION

Experimental setup for continuous Li extraction via RCE

The experimental setup for the continuous Li extraction via RCE is illustrated in Figures 2A and S1. The RCE system consists of three compartments: the feed compartment, the extraction compartment, and the collection compartment. Within the feed compartment, two syringe pumps flow the Li-rich brine and the receiving solution into the extraction compartment for Li extraction. The core component in the extraction compartment is a flow cell, which is constructed by stacking acrylic frames with gas diffusion electrodes (GDEs) and SSE membrane to form the gas and liquid chambers (Figure 2B). The spent brine and enriched solution from the flow cell are collected in the collection compartment for further characterizations.

In the RCE system, the Li-selective membrane is a crucial element, given its profound impact on Li transport dynamics. In this work, we use the NASICON-type LAGP as the Li-selective membrane due to its high Li conductivity[22] and selectivity[23] at room temperature. Most important, LAGP presents excellent stability in mixed aqueous solutions containing Li, Na, K, and Mg ions. The thermodynamically stable crystal structure of LAGP specific to Li prevents ion exchange between the embedded Li in LAGP and other ions,[23] such as Na and K. This stability serves as the foundation for consistent and long-term Li extraction. The fabrication of the LAGP membrane incorporates traditional sintering techniques, where LAGP

Please cite this article in press as: Xu et al., Continuous lithium extraction from brine by efficient redox-couple electrodialysis, Matter (2024), https://doi.org/10.1016/j.matt.2024.07.014

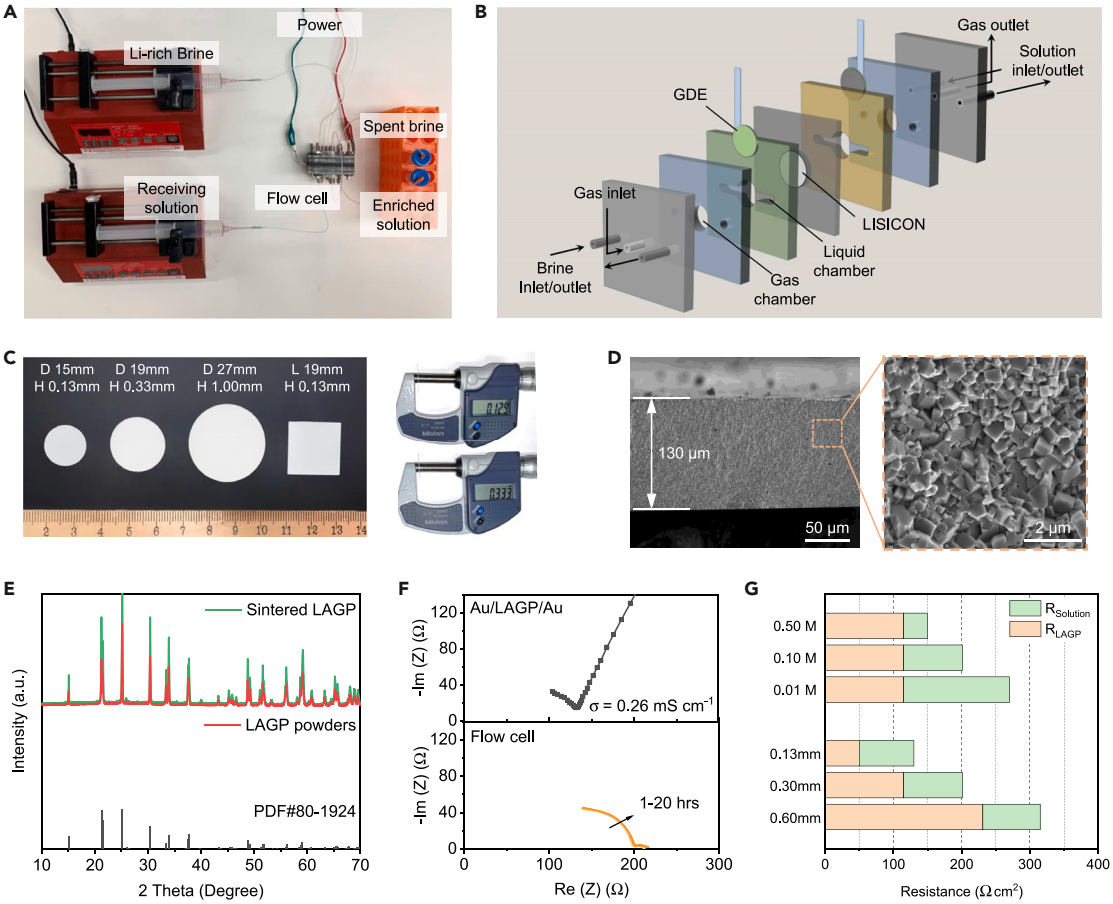

Figure 2. Experimental setup for continuous Li extraction via RCE

(A) Experimental apparatus for continuous Li extraction.

(B) Schematic of the flow cell for electrodialysis.

(C) The LAGP membranes with varied dimensions. D, diameter; H, thickness; L, side length of a square.

(D) SEM images highlighting the cross-sectional microstructure of the LAGP membrane.

(E) XRD patterns of the pristine LAGP powder and the sintered LAGP membrane.

(F) EIS spectra of the LAGP membrane (top) and the flow cell (bottom).

(G) Resistance analysis for the flow cell with the LAGP membranes of different thicknesses and with varied Li solution concentrations.

powders are first cold-pressed into a green body and then sintered in the furnace without pressure. This methodology offers scalability for the mass production of LAGP membranes of varying sizes and thicknesses (Figure 2C). Cross-sectional scanning electron microscopy (SEM) images of the sintered LAGP membrane reveal its low porosity (Figure 2D), which aligns well with its high relative density of 95.0% measured by the Archimedes method. X-ray diffraction (XRD) patterns validate that the sintered LAGP membrane retains the same crystalline composition as the pristine LAGP powders (Figure 2E). Relying on the electrochemical impedance spectroscopy (EIS) spectra measured from the Au/LAGP/Au blocking cell (Figure 2F), we calculated the ionic conductivity of LAGP as 0.26 mS cm^{-1} at room temperature, which agreed well with previous reports (0.2 mS cm^{-1}).[22]

Before initiating the Li extraction from brine, we need to evaluate the electrochemical stability of the flow cell. Following a 20-h settling/forming period, the EIS spectra of the flow cell exhibit negligible variation (Figure 2F, bottom), suggesting that the cell remains undegraded from the solution leakage or membrane corrosion. The

Please cite this article in press as: Xu et al., Continuous lithium extraction from brine by efficient redox-couple electrodialysis, Matter (2024), https://doi.org/10.1016/j.matt.2024.07.014

calculated resistance of the flow cell is predominantly shaped by two factors: the Li transport through the LAGP membrane and through the LiOH solution. By tuning the thickness of the LAGP membrane (e.g., 0.13, 0.30, and 0.60 mm) and the Li concentration in the solution (e.g., 0.01, 0.10, and 0.50 M), we can manipulate the resistance associated with Li transport through these media (Figures 2G and S2). It also implies that potential reductions in resistance (or operational voltage) for Li extraction can be achieved by tuning these two factors.

Continuous Li extraction from Li-rich brine via RCE

We first assessed the efficacy of the continuous Li extraction from the brine with a Li concentration of 70 ppm (0.01 M) and Na concentration of 2,300 ppm (0.1 M). This composition closely mirrors that in the oil-extraction brine (~100 ppm).[24] The flow rate of the brine and receiving solution entering the extraction compartment is set at 4 cm h^{-1}, and the applied current density for Li extraction is fixed at 0.08 mA cm^{-2}. This operating condition would, theoretically, enable the extraction of 75% of Li from the brine (indicated by the black dashed line in Figure 3A) to enrich the receiving solution (0.01 M LiOH). In practice, the Li concentration in the brine drops from an initial 70 ppm to a stable state of about 25 ppm after the 2-h Li extraction and remains stable thereafter (Figure 3A). Correspondingly, the Li ions extracted from the brine enrich the receiving solution, as confirmed by the increased Li concentration in the receiving side (Figure 3B). Notably, Na concentrations on both sides remain relatively stable, emphasizing the high Li selectivity of the RCE approach so that Na ions are not transferred from the brine to the receiving solution. More important, throughout the Li extraction, the operating voltage is impressively low at ~45 mV, and the faradaic efficiency and Li selectivity remain at a high level of 85.5% and 0.9920 (averaged over the 2–10 h period), respectively (Figure 3C).

Per literature reports, Li-rich brines can contain Li ions with varying concentrations. For example, the Li concentration ranges from 180 to 250 ppm in the brine at Clayton Valley (Nevada, USA)[25] and is about 690 ppm in the brine at Salar de Olaroz (Jujuy, Argentina).[26] Here, we evaluated the performance of Li extraction from the Li-rich brines with different Li concentrations (70, 210, and 630 ppm). The Na concentration in these brines is maintained at 2,600 ppm. The faradaic efficiency and Li selectivity during the Li extraction from these varied-concentration brines are consistently high, ranging from 85% to 90% and 0.990 to 0.999, respectively (Figures 3D and S3). This indicates that only a small amount of the electricity (10%–15%) is lost due to the potential Li loss carried by the brine flowing and the side reactions at the electrode-electrolyte interface. In general, a higher Li concentration enhances the extraction efficiency and selectivity, which aligns well with most results reported in the literature.[7] To explore the feasibility of our electrodialysis method in extracting Li from the brine with higher Na concentration, we tested the performance of continual Li extraction from the brine with an Li concentration of 210 ppm and an Na concentration of 23,000 ppm. The driving force for extracting Li from the brine to the supporting solution increases from 0.25–0.30 to 0.7–0.75 V when the brine present higher salinities (Figure S4). Despite this increase, the voltage required for Li extraction remains much lower compared to most electrochemical Li extraction techniques (3–10 V; Figure 3G). Similarly, the faradaic efficiency and Li selectivity show slight declines but remain within a reasonable range of 70.52% and 98.53%, respectively (Figure S4).

Additionally, we evaluated the performance of Li extraction under various operating conditions, specifically focusing on the applied current density and the flow rate of feeding brine. Holding the Li concentration in the brine at 210 ppm and the flow rate of feeding brine at 4 cm h^{-1}, we obtained the faradaic efficiency and Li selectivity of

Please cite this article in press as: Xu et al., Continuous lithium extraction from brine by efficient redox-couple electrodialysis, Matter (2024), https://doi.org/10.1016/j.matt.2024.07.014

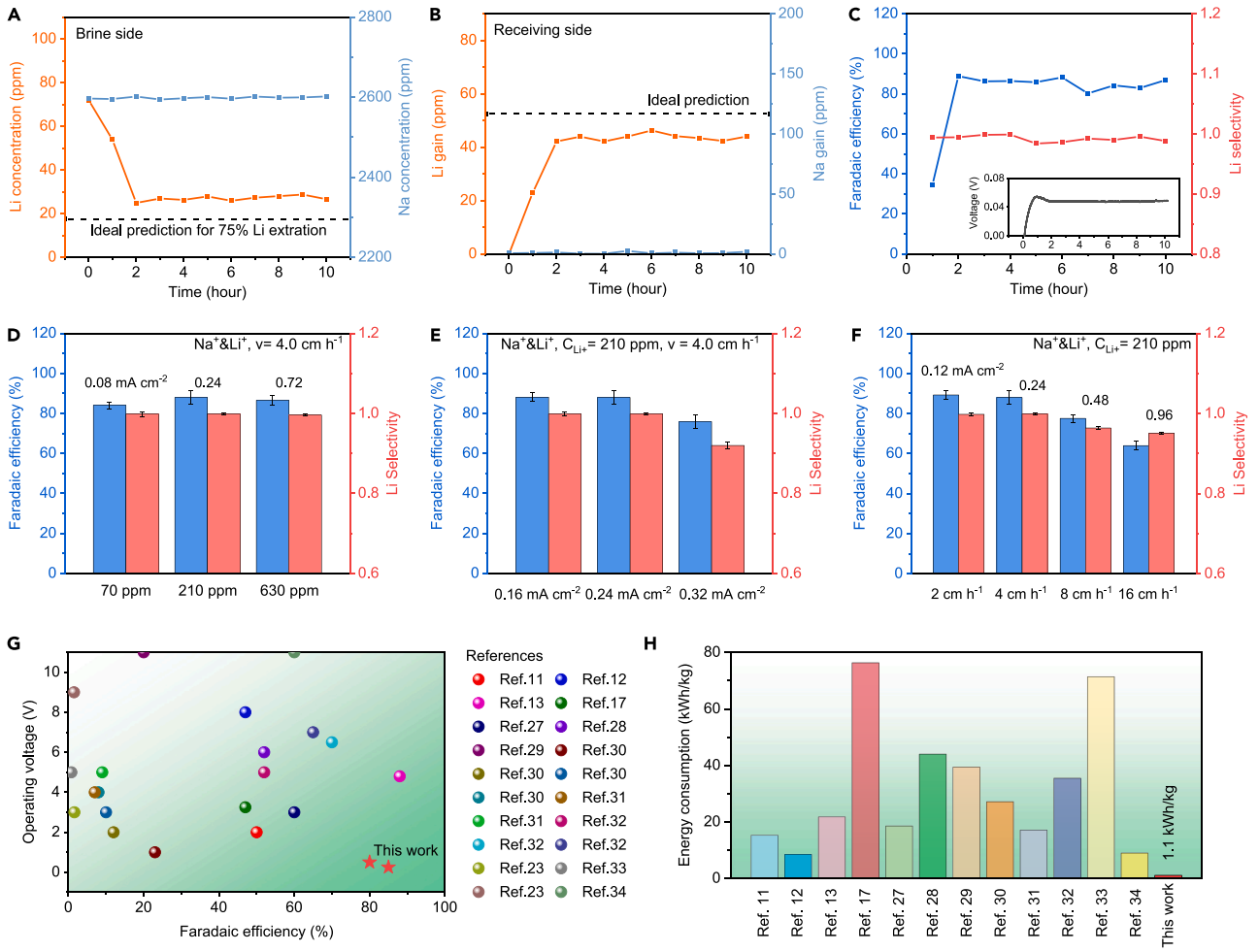

Figure 3. Continuous Li extraction from Li-rich brine

(A and B) Time-evolving concentrations of Li and Na in the brine (A) and the receiving solution (B) during Li extraction.

(C) Voltage, faradaic efficiency, and Li selectivity of continuous Li extraction.

(D) Faradaic efficiency and Li selectivity of the Li extraction from the brine with different initial Li concentrations. Error bars are calculated based on the 2–10 h Li extraction period.

(E and F) Faradaic efficiency and Li selectivity of the Li extraction under different applied current densities (E) and brine flow rates (F). Error bars are calculaed based on the 2–10 h Li extraction period.

(G and H) Summary of operating voltage. Faradaic efficiency plot (G) and energy consumption plot (H) for the RCE approach and the reported electrochemical DLE prototypes.[11–13,17,27–34]

the Li extraction under three different current densities: 0.16, 0.24, and 0.32 mA cm^{-2}. These current densities correspond to the extraction of 50%, 75%, and 100% of the Li content in the brine, respectively. For current densities of 0.16 and 0.24 mA cm^{-2}, the faradaic efficiency and Li selectivity remained relatively constant at about 85% and 0.99, respectively (Figures 3E and S5). For a current density of 0.32 mA cm^{-2}, we observed a slight decrease to 76% in faradaic efficiency and 0.92 in Li selectivity. A similar trend is noticed when increasing the flow rate (Figures 3F and S6). However, for brine with an Li concentration of 630 ppm, the current density for Li extraction can reach up to 2.0 mA cm^{-2} (Figure S7), under which the faradaic efficiency and Li selectivity are 74% and 0.982, respectively.

To illustrate the advantages of our RCE approach, we also compared its operating voltage and faradaic efficiency with previously reported DLE techniques (Figure 3G).

Please cite this article in press as: Xu et al., Continuous lithium extraction from brine by efficient redox-couple electrodialysis, Matter (2024), https://doi.org/10.1016/j.matt.2024.07.014

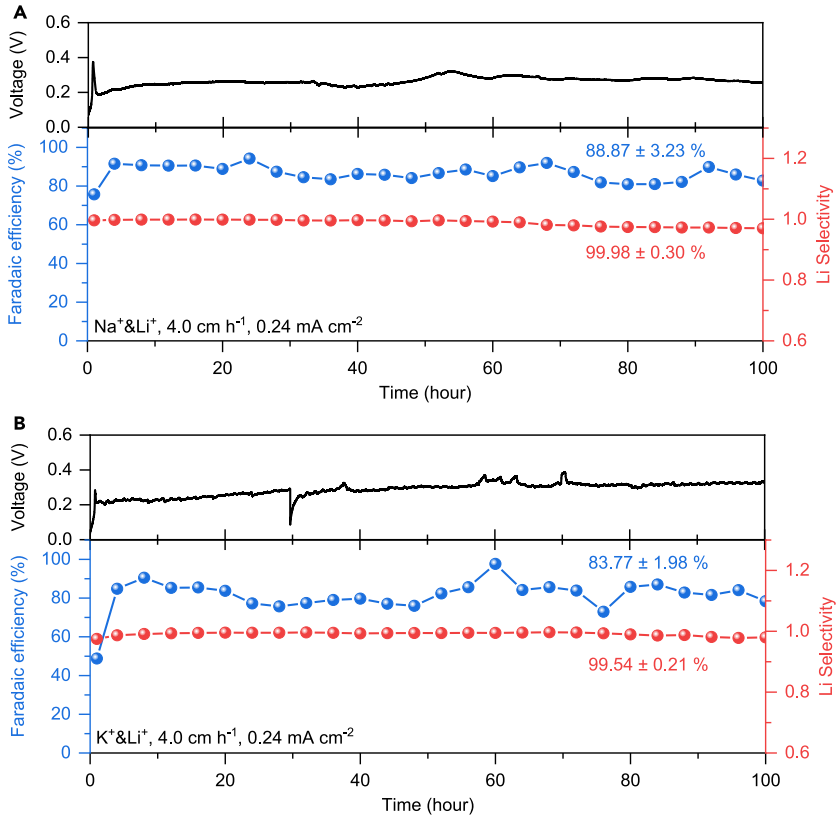

Figure 4. Long-term stability of continuous Li extraction

The voltage, faradaic efficiency, and Li selectivity during long-term continuous Li extraction from the brine with mixed Li/Na ions (A) and Li/K ions (B).

Generally, the operating voltage for most DLE techniques falls in the range of 2.0–6.0 V, with faradaic efficiency lower than 70%. However, by employing the redox couple HER/HOR, the Li extraction via RCE manages to reduce the operating voltage to below 0.5 V while maintaining the faradaic efficiency above 80%, resulting in an impressively low specific energy consumption. For instance, under 0.48 mA cm^{-2} and 8 cm h^{-1}, the Li extraction from the brine with an Li concentration of 210 ppm operates at a rate comparable with the most state-of-the-art DLE techniques (Figure S8), while it only consumes specific energy of a mere 1.1 kWh kg_{Li}^{-1} (equivalent to 0.105 kWh kg_{LCE}^{-1}), approximately an order of magnitude lower than most reported DLE techniques (Figure 3H).[11–13,17,27–34] Such reduced energy consumption significantly enhances the feasibility of implementing our RCE approach in practical large-scale applications.

We last examined the long-term performance of the continuous Li extraction from the brine-containing mixed ions—specifically, blends of Li and Na ions and blends of Li and K ions. Operating under 4 cm h^{-1} and 0.24 mAh cm^{-2}, the Li extraction from the Li-Na mixed brine presents good stability over 100 h (Figure 4A). The voltage shows a plateau around 0.25 V, and the average faradaic efficiency and Li selectivity reach as high as 88.87% and 0.9998, respectively. In parallel, our RCE approach also exhibits promising efficacy when applied to the brine with Li and K mixed ions (Figure S9). Maintaining the same flow rate and current density, the faradaic efficiency and Li selectivity of Li extraction remain commendably high, at 83.77% and 0.9954, respectively (Figure 4B). More important, when the device scale

Please cite this article in press as: Xu et al., Continuous lithium extraction from brine by efficient redox-couple electrodialysis, Matter (2024), https://doi.org/10.1016/j.matt.2024.07.014

is amplified by 4 times, the performance of continuous Li extraction remains outstanding where the faradaic efficiency and Li selectivity are 92.4% and 0.9940, respectively (Figure S10).

Stability of LAGP membranes during continuous Li extraction

In this section, we evaluate the electrochemical stability of the LAGP membrane during Li extraction via postmortem analysis and numerical simulations. Two LAGP membranes after 20-h Li extraction are collected and rinsed by deionized water for evaluation: one under a low current density and flow rate (0.24 mA cm^{-2} and 4 cm h^{-1}) and the other under a high current density and flow rate (0.96 mA cm^{-2} and 16 cm h^{-1}). After operating under a low current density and flow rate, the surface of the LAGP membrane in contact with brine exhibits very little change compared to its pristine state (Figures 5A and 5B). However, the post-operation LAGP exposed to a higher current density and flow rate showcases an apparent microstructural evolution only at the surface in contact with brine (Figure S11), where the initially dense-packed LAGP gains lose contact with one another, resulting in the increased porosity at the LAGP surface (Figures 5C and 5D). Such morphological evolution indicates the structural degradation of LAGP membranes after long-term exposure to the brine under aggressive operational conditions.

The evolution in surface morphology and composition is further supported by XRD and X-ray photoelectron spectroscopy (XPS) analysis (Figures 5E–5G). Operation under high current density significantly reduces the LAGP crystallinity, as validated by the weakened XRD intensity and the merging of diffraction peaks, such as (211) and (116) orientations (Figure 5E). The XPS spectra for the Na signal (Figure 5F), combined with the calculated element ratio of Na/P (Figures 5G and S12), imply the infiltration of Na ions into the LAGP surface, likely through the replacement of Li ions by the larger Na ions. The volume mismatch associated with the Li-Na ion exchange can induce the structural degradation of LAGP membranes (Figure 5C), such as microcracks, increased porosity, and reduced crystallinity.

To better understand the structural evolution of LAGP during Li extraction, we perform numerical simulations to visualize the dynamic ion transport in the flow cell. Figure 5H illustrates the Li distribution within the flow cell during the Li extraction at varied current densities. The left domain represents the cross-sectional view of the Li brine chamber, and the right domain is for the receiving solution chamber (Figure S13). Under a lower current density and flow rate (left panel in Figures 5H and S14), Li ions in most parts of the brine chamber can transport through the LAGP membrane to the receiving side, as indicated by the uniform light blue color (low Li concentration) of the spent brine flowing out at the top boundary. However, under a higher current density (right panel in Figures 5H and S14), only the Li ions near the LAGP membrane can be transported to the receiving side, leading to local ion depletion in the brine, as highlighted by the dark blue region.

The temporal evolution of the Li concentration along the outflow boundary (Figures 5I, S15, and S16) further shows an increase in the Li concentration gradient in the brine when the current density and flow rate are amplified. In this context, the Li ions far from the LAGP membrane cannot traverse through the chamber thickness fast enough before being carried out by the flow. Such a phenomenon leads to a high residual concentration of Li ions in the brine, which negatively affects the measured faradaic efficiency of the Li extraction under aggressive operating conditions (Figure 3F). Meanwhile, to maintain charge balance, Na ions are forced to insert into the LAGP at the Li depletion region (Figure 5J), potentially damaging the

Please cite this article in press as: Xu et al., Continuous lithium extraction from brine by efficient redox-couple electrodialysis, Matter (2024), https://doi.org/10.1016/j.matt.2024.07.014

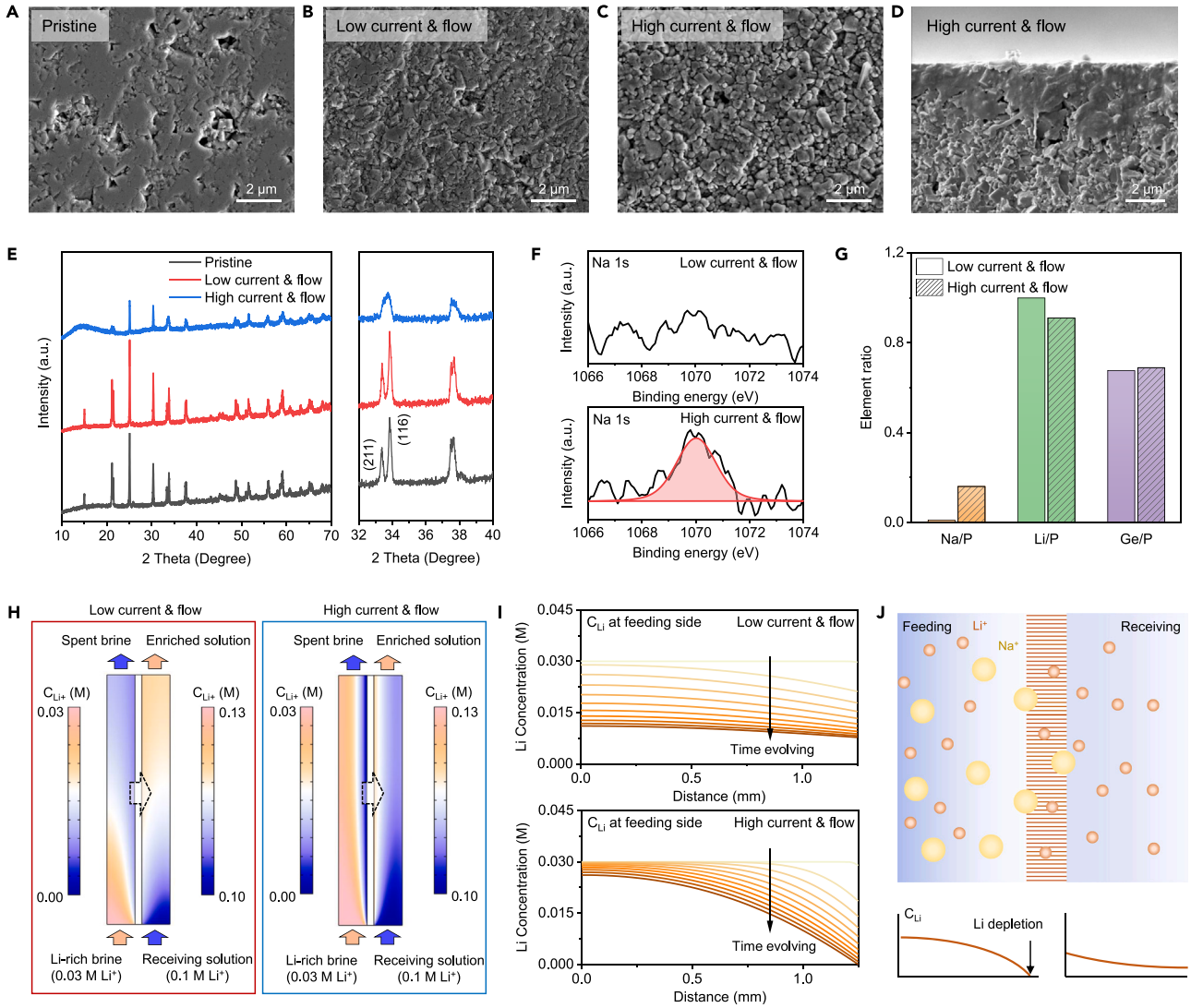

Figure 5. Characterizations of post-operation LAGP membranes

(A–D) SEM images of the LAGP membranes before (A) and after (B–D) the 20-h Li extraction. (A)–(C) show the top view of the LAGP surface in contact with the brine, and (D) shows the cross-section view with the upper surface in contact with the brine.

(E and F) XRD patterns (E) and XPS spectra (F) of the LAGP operating for 20-h Li extraction under the low (0.24 mA cm^{-2}) and high (0.96 mA cm^{-2}) current densities. Both the XRD patterns and XPS spectra are taken at the surface of the LAGP membrane in contact with brine.

(G) Element ratio deduced from the XPS spectra.

(H) Numerical simulation visualizing the Li distribution in the flow cell during the Li extraction at varied current densities.

(I) Evolution of Li concentration in the brine side during the Li extraction under varied current densities.

(J) Schematic illustrating the Li depletion near the brine/LAGP interface under a high current density.

structural integrity of LAGP membranes (Figures 5C and 5E). Given these insights, it becomes unequivocal that optimizing the flow cell design to balance the mass transport of Li, the flow rate of fluids, and the applied current density is paramount for future improvements in the system stability for practical applications (i.e., further increase of the current densities up to ~10 mA cm^{-2}). For example, by depositing a layer of TiO_2 (6 nm) on the surface of the LAGP membrane via atomic layer deposition, we find that the faradaic efficiency and Li selectivity increase from 65% to 74% and from 0.951 to 0.979, respectively, under the current densities of 0.96 mA cm^{-2} (Figure S17).

Please cite this article in press as: Xu et al., Continuous lithium extraction from brine by efficient redox-couple electrodialysis, Matter (2024), https://doi.org/10.1016/j.matt.2024.07.014

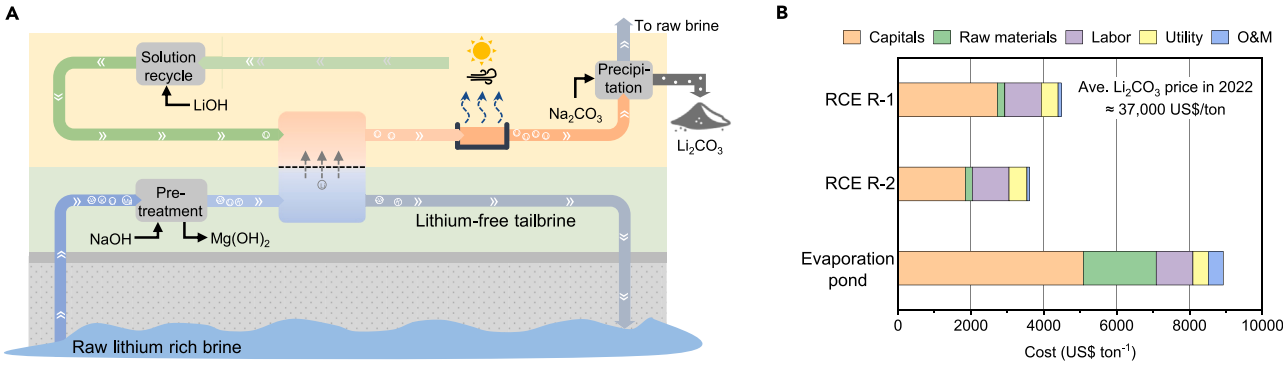

Figure 6. Techno-economic analysis of continuous Li extraction via RCE

(A) A full process train for the continuous Li extraction from the brine via RCE.

(B) Techno-economic analysis of two RCE routes, compared against conventional Li mining through evaporation and chemical precipitation. Complete data compilation is provided in Table S2.

Techno-economic analysis of continuous Li extraction via RCE

A preliminary techno-economic analysis is conducted to demonstrate the economic feasibility of continuous Li extraction via RCE. The cost to deliver the targeted production Li_2CO_3 is selected as the economic metric, where the route with the lower cost is more economically profitable. Two routes of RCE, R-1 and R-2, are designed based on the full process train for the continuous Li extraction via RCE (Figure 6A). For RCE R-1, the applied current density and flow rate are set at 0.24 mA cm^{-2} and 4 cm h^{-1}, respectively. For RCE R-2, these values are 0.48 mA cm^{-2} and 8 cm h^{-1}, respectively. The route of the evaporation pond represents the process train for conventional Li mining via evaporation and chemical precipitation (route evaporation pond, Figure S18), serving as the benchmark for the techno-economic analysis. The total cost (unit: US dollars per metric ton of LCE) for Li mining via each proposed train is the cumulative sum of capital expenses, raw material costs, labor wages, operating and maintenance (O&M) costs, and utilities. A detailed description of the specific assumptions and costing methodologies for each unit process is provided in Table S1 and the supplemental notes.

Conventional Li extraction involves the construction of large-scale solar evaporation ponds to concentrate the Li in the raw brine. The substantial construction cost (US$64 m^{-2}, as reported by Mickley and Associates)[35] significantly escalates both capital and O&M costs for Li extraction. By contrast, the need for evaporation ponds is eliminated in the RCE process, thereby reducing capital costs from US$5,087 ton^{-1} to US$2,731 ton^{-1} for RCE R-1 and further down to US$1,850 ton^{-1} for RCE R-2 (Figure 6B). Additionally, the Li extraction via RCE bypasses the requisite for sizable quantities of reagents, which alone contributed to a 36% total cash cost for conventional Li mining in 2019. As a result, raw material costs drop from US$2,000 ton^{-1} to US$200 ton^{-1} for RCE-R1 (US$190 ton^{-1} for RCE R-2). Moreover, the Li extraction via RCE consumes a small amount of energy due to its low operating voltages, thereby avoiding the burden of extra electricity cost (US$25 ton^{-1} for RCE R-1 and US$60 ton^{-1} for RCE R-2). In conclusion, the RCE routes offer a substantially reduced cost profile (US$4,410 ton^{-1} for RCE R-1 and US$3,543 ton^{-1} for RCE R-2) compared to conventional Li extraction methods (US$9,119 ton^{-1}), making it notably competitive against the prevailing market prices of Li products (US$37,000 ton^{-1}).[36] The costs of Li extraction could be further reduced when adopting even higher current densities and flow rates, positioning the RCE technique as a promising avenue for efficient and cost-effective Li production from brines.

Please cite this article in press as: Xu et al., Continuous lithium extraction from brine by efficient redox-couple electrodialysis, Matter (2024), https://doi.org/10.1016/j.matt.2024.07.014

Conclusions

In summary, we introduce a highly efficient RCE approach to realize sustainable Li extraction from oil extraction and salt-lake brines. Our design leverages the redox couple—HER and HOR—as the driving force for electrodialysis, which minimizes consumption energy because of their low overpotential and equilibrium potential. Meanwhile, the integration of SSEs serving as Li-ion selective membranes ensures high selectivity when extracting Li from mixed-ion brines. We demonstrate a continuous Li extraction from brines for over 100 h, with an operating voltage of around 0.25 V, an average faradaic efficiency of 88.87%, and an average Li selectivity of 0.9954. Notably, the Li extraction via RCE only consumes a specific energy of 1.1 kWh kg_{Li}^{-1}, approximately an order of magnitude lower than the energy demands of most reported Li extraction techniques. Preliminary techno-economic analysis reveals that the Li extraction via RCE offers a substantially reduced cost (US$4,410 ton^{-1}) compared to traditional Li extraction via evaporation and chemical precipitation (US$9,119 ton^{-1}), as the RCE approach eliminates the construction of large-scale solar evaporation ponds and the requisite for substantial quantities of reagents. These advantages displayed by the RCE approach over traditional Li extraction techniques enhance its feasibility in eco-friendly and cost-effective Li production, with broad implications for the electrified transportation and renewable energy storage industries.

EXPERIMENTAL PROCEDURES

Resource availability

Lead contact

All queries about experimental procedures can be directed to the lead contact, Yi Cui (yicui@stanford.edu).

Materials availability

This study did not generate new unique reagents. All relevant vendors and synthesis procedures are included in the following sections from "preparation of LAGP membrane" to "flow cell assembly and direct Li extraction" and in the supplemental information.

Data and code availability

All relevant data are included in the paper and the supplemental information.

Preparation of LAGP membrane

LAGP powder was purchased from MSE Supplies. The LAGP powder was pressed into a green pellet using a die set under constant uniaxial pressure of 200 MPa for 1 min. The green pellet was sintered at 850°C for 6 h in a muffle furnace. The sintered LAGP pellets were around 15.0 mm in diameter. Before further testing, the pellets were first polished with 500-, 1,000-, and 2,000-grit SiC sandpaper using a Buehler EcoMet250 polisher.

Material characterization

XRD (PANalytical Empyrean with a Cu(Kα) X-ray source) was utilized to examine the phase purity of the LAGP membrane. Diffraction patterns were collected from 10° to 70° using a step size of 0.01°. Microstructural analysis was performed using a scanning electron microscope (Thermo Fisher Scientific Apreo). An energy-dispersive X-ray detector (XFlash 6 | 60 Silicon Drift Detector) integrated into the scanning electron microscope was used to map the elemental distributions. XPS (PHI VersaProbe I with a monochromatized Al(Kα) X-ray source) was used to characterize the surface chemical compositions for the LAGP membrane. The ionic conductivity of LAGP

Please cite this article in press as: Xu et al., Continuous lithium extraction from brine by efficient redox-couple electrodialysis, Matter (2024), https://doi.org/10.1016/j.matt.2024.07.014

membranes was determined by the EIS (Biologic VMP3 system), with a frequency range from 1 MHz to 0.1 Hz and a perturbation voltage of 10 mV at room temperature. The Au/LAGP/Au blocking cells for EIS measurement were prepared by sputtering thin Au layers (50 nm) on both surfaces of the LAGP pellets as two electrodes. The EIS spectra were fit to an equivalent circuit containing two RC components in series representing the bulk and interfacial resistances.

Flow cell assembly and direct Li extraction

The flow cell components were fabricated from the acrylic sheet using the laser cutter Epilog Fusion M2. GDEs purchased from the Fuel Cell Store were used as the anode and cathode. The catalyst loading on the carbon cloth electrodes was 0.2 mg cm^{-2} (80% carbon + 20% Pt). The exposed areas of LAGP, cathode, and anode are designed as 1 cm^2 each. The thickness of the LAGP used for Li extraction is fixed at 0.3 mm. The flow cell components were assembled with rubber gaskets between each component and tightened by stainless-steel bolts and nuts. The feeding solution was 0.1 M NaCl and 0.01 M (or 0.03 and 0.1 M) LiOH; the receiving solution was 0.1 M LiOH. The feeding and receiving solutions are each connected to a syringe pump (1000-US, SyringeONE) for flow rate adjustments. The flow rate of the feeding solution (cm h^{-1}) is used to control the Li extraction rate, as it is a critical parameter determining the performance of Li extraction. The flow rate can be calculated by dividing the volume rate of the feeding solution (mL h^{-1}) by the cross-sectional area of the flow (cm^2). For the flow cell design shown in Figure S1, a flow rate of 4 cm h^{-1} is equivalent to a volume rate of 0.4 mL h^{-1}. After passing through the flow cell, the spent feeding solution and enriched receiving solution were collected from the flow cell and diluted with a 1% aqueous nitric acid solution for inductively coupled plasma mass spectrometry analysis (Thermo Scientific XSERIES 2 Quadrupole).

Calculation of the faradaic efficiency, Li selectivity, and energy consumption

The faradaic efficiency was calculated by

$$\text{Faradaic efficiency} = \frac{ZFV\Delta C_{Li^+}}{Q},$$

where Z is the charge number of the Li ion, F is the Faraday constant, V is the total volume of feeding solution flowing through the cell, ΔC_{Li^+} is the variation of Li ion concentration in the receiving solution, and Q is the charge consumption. The nominal Li selectivity was calculated by

$$\text{Li selectivity} = \frac{\Delta C_{Li^+}}{(\Delta C_{Li^+} + \Delta C_{Na^+})},$$

where ΔC_{Na^+} is the variation of Na-ion concentration in the receiving solution. The energy consumption is calculated by

$$\text{Energy consumption} = \frac{QU}{V\Delta C_{Li^+} M_{Li^+}},$$

where U is the average applied voltage and M_{Li^+} is the molecular weight of Li ions.

Numerical simulation

The numerical simulations on the ion transport in the solution and through the LAGP membrane are performed using the tertiary current distribution with the Nernst-Planck electroneutrality model integrated in the COMSOL Multiphysics software. The migration, diffusion, and convection of ions (Li^+, Na^+, K^+, OH^-) in the solution are governed by the Nernst-Planck equation,

$$\frac{\partial C_i}{\partial t} + \nabla \cdot \mathbf{J}_i = 0$$

$$\mathbf{J}_i = -D_i \nabla C_i + C_i \mathbf{v} - \frac{z_i D_i F C_i \nabla \phi_l}{RT},$$

where C_i is the ion concentration, D_i is the diffusivity of ions, $\mathbf{v}$ is the velocity vector of the solution, z_i is the charge of ions, F is the Faraday constant, ϕ_l is the electrolyte potential, R is the molar gas constant, and T is the temperature. The subscript i represents the different ion species ($i = Li^+$, Na^+, K^+, OH^-). The distribution of electrolyte potential in the LAGP is solved by the Laplace equation,

$$\nabla \cdot \mathbf{i}_m = 0$$

$$\mathbf{i}_m = -\sigma_m \nabla \phi_m,$$

where $\mathbf{i}_m$ is the current density in the LAGP, σ_m is the ionic conductivity of LAGP, and ϕ_m is the electrolyte potential in LAGP. The interfaces between the solution and LAGP membrane are described by the continual boundaries with Donnan conditions,[37]

$$\phi_l - \phi_m = -\frac{RT}{z_{Li}F} \ln\left(\frac{C_{Li}}{C_m}\right),$$

where C_m is the Li concentration in LAGP. The geometries and boundary conditions of the two-dimensional simplified model are set to be consistent with the experimental setups (Figures S1 and S11). The materials and physical properties used in the numerical simulation are summarized in Table S3.

Techno-economic analysis

Spreadsheet models are built to perform the techno-economic analysis of the proposed routes. The process train of the evaporation pond represents the processes for conventional Li mining via evaporation and chemical precipitation (Figure S15), serving as the baseline case for the techno-economic analysis. Two routes of RCE (RCE-R1 and RCE-R2) are established based on the full process train for the continuous Li extraction from brine (Figure 6A). The current density and flow rate in the RCE R-1 are assumed to be 0.24 mA cm^{-2} and 4 cm h^{-1}, respectively, while the current density and flow rate in the RCE R-2 are assumed to be 0.48 mA cm^{-2} and 8 cm h^{-1}, respectively. The total cost for Li mining (unit: US dollars per metric ton of LCE) through all the proposed trains consists of capital expenses, raw material costs, labor wages, O&M costs, and utilities. The capital cost is calculated using a model developed in previous works,[38] where the local evaporation rate and the volume of the brine for treatment are used to determine the required size of the evaporation pond and the construction fee. The costs of raw materials are obtained from the market and consumer data 2022 by Statista Inc. (Table S1). The labor fees and O&M costs were calculated by data reported in previous works.[28] For all routes, it is assumed that Li extraction plants are located near the brine sources, so the cost of pumping the Li-containing brine and the transportation of products and by-products is ignored. Royalty costs for brine operations are also ignored, as these costs can vary significantly, depending on the geographic location and local policies. A detailed description of the specific assumptions and costing methodologies for each unit process is provided in Table S1 and the supplemental notes.

SUPPLEMENTAL INFORMATION

Supplemental information can be found online at https://doi.org/10.1016/j.matt.2024.07.014.

ACKNOWLEDGMENTS

Part of this work was performed at the Stanford Nano Shared Facilities (SNSF), supported by the National Science Foundation under award ECCS-2026822. Part of this work was performed in the nano@Stanford labs, supported by the National Science Foundation as part of the National Nanotechnology Coordinated Infrastructure under award ECCS-1542152. This work was supported by the Stanford StorageX Initiative.

AUTHOR CONTRIBUTIONS

R.X. and Y.C. conceived the idea for the study. R.X., P.Z., and S.B.C. conducted the sample fabrication and processing. R.X., Y. Ye, and Y. Yang performed the material characterizations. R.X., X.X., and G.Z. performed the electrochemical test and data analysis. R.X. performed the numerical analysis and techno-economic analysis. R.X. and Y.C. wrote and revised the manuscript. All authors contributed to the discussion of the manuscript.

DECLARATION OF INTERESTS

The authors declare no competing interests.

Received: February 12, 2024
Revised: June 28, 2024
Accepted: July 22, 2024
Published: August 21, 2024

REFERENCES

1. Azevedo, M., Baczyńska, M., Hoffman, K., and Krauze, A. (2022). Lithium mining: How new production technologies could fuel the global EV revolution. https://www.mckinsey.com/industries/metals-and-mining/our-insights/lithium-mining-how-new-production-technologies-could-fuel-the-global-ev-revolution.

2. Song, J.F., Nghiem, L.D., Li, X.-M., and He, T. (2017). Lithium extraction from Chinese salt-lake brines: opportunities, challenges, and future outlook. Environ. Sci. Water Res. Technol. *3*, 593–597. https://doi.org/10.1039/C7EW00020K.

3. Flexer, V., Baspineiro, C.F., and Galli, C.I. (2018). Lithium recovery from brines: A vital raw material for green energies with a potential environmental impact in its mining and processing. Sci. Total Environ. *639*, 1188–1204. https://doi.org/10.1016/j.scitotenv.2018.05.223.

4. Kaunda, R.B. (2020). Potential environmental impacts of lithium mining. J. Energy Nat. Resour. Law *38*, 237–244. https://doi.org/10.1080/02646811.2020.1754596.

5. Vera, M.L., Torres, W.R., Galli, C.I., Chagnes, A., and Flexer, V. (2023). Environmental impact of direct lithium extraction from brines. Nat. Rev. Earth Environ. *4*, 149–165. https://doi.org/10.1038/s43017-022-00387-5.

6. Xiong, Y., Zhou, J., Lu, P., Yin, J., Wang, Y., and Fan, Z. (2022). Electrochemical lithium extraction from aqueous sources. Matter *5*, 1760–1791. https://doi.org/10.1016/j.matt.2022.04.034.

7. Liu, C., Li, Y., Lin, D., Hsu, P.C., Liu, B., Yan, G., Wu, T., Cui, Y., and Chu, S. (2020). Lithium Extraction from Seawater through Pulsed Electrochemical Intercalation. Joule *4*, 1459–1469. https://doi.org/10.1016/j.joule.2020.05.017.

8. Zhao, M.Y., Ji, Z.Y., Zhang, Y.G., Guo, Z.Y., Zhao, Y.Y., Liu, J., and Yuan, J.S. (2017). Study on lithium extraction from brines based on $LiMn_2O_4/Li_{1-x}Mn_2O_4$ by electrochemical method. Electrochim. Acta *252*, 350–361. https://doi.org/10.1016/j.electacta.2017.08.178.

9. Hu, J., Jiang, Y., Li, L., Yu, Z., Wang, C., Gill, G., Xiao, J., Cavagnaro, R.J., Kuo, L.J., Asmussen, R.M., and Lu, D. (2022). A Lithium Feedstock Pathway: Coupled Electrochemical Extraction and Direct Battery Materials Manufacturing. ACS Energy Lett. *7*, 2420–2427. https://doi.org/10.1021/acsenergylett.2c01216.

10. Xiong, J., Zhao, Z., Liu, D., and He, L. (2022). Direct lithium extraction from raw brine by chemical redox method with $LiFePO_4/FePO_4$ materials. Sep. Purif. Technol. *290*, 120789. https://doi.org/10.1016/j.seppur.2022.120789.

11. Hoshino, T. (2015). Innovative lithium recovery technique from seawater by using world-first dialysis with a lithium ionic superconductor. Desalination *359*, 59–63. https://doi.org/10.1016/j.desal.2014.12.018.

12. Qiu, Y., Yao, L., Tang, C., Zhao, Y., Zhu, J., and Shen, J. (2019). Integration of selectrodialysis and selectrodialysis with bipolar membrane to salt lake treatment for the production of lithium hydroxide. Desalination *465*, 1–12. https://doi.org/10.1016/j.desal.2019.04.024.

13. Yang, S., Zhang, F., Ding, H., He, P., and Zhou, H. (2018). Lithium Metal Extraction from Seawater. Joule *2*, 1648–1651. https://doi.org/10.1016/j.joule.2018.07.006.

14. Manthiram, A., Yu, X., and Wang, S. (2017). Lithium battery chemistries enabled by solid-state electrolytes. Nat. Rev. Mater. *2*, 16103–16116. https://doi.org/10.1038/natrevmats.2016.103.

15. Jiang, Z., Kong, W., Zhao, F., Han, Q., Liu, Y., Wang, S., and Wang, H. (2023). $Li_{1.5}Al_{0.5}Ge_{1.5}(PO_4)_3$ membrane electrodialysis for lithium enrichment. J. Membr. Sci. *670*, 121353. https://doi.org/10.1016/j.memsci.2023.121353.

16. Shen, K., He, Q., Ru, Q., Tang, D., Oo, T.Z., Zaw, M., Lwin, N.W., Aung, S.H., Tan, S.C., and Chen, F. (2023). Flexible LATP composite membrane for lithium extraction from seawater via an electrochemical route. J. Membr. Sci. *671*, 121358. https://doi.org/10.1016/j.memsci.2023.121358.

17. Li, Z., Li, C., Liu, X., Cao, L., Li, P., Wei, R., Li, X., Guo, D., Huang, K.W., and Lai, Z. (2021). Continuous electrical pumping membrane process for seawater lithium mining. Energy Environ. Sci. *14*, 3152–3159. https://doi.org/10.1039/D1EE00354B.

18. Huang, H., Li, Z., Li, Z., Khan, B., Huang, K.W., Lai, Z., and He, J.H. (2023). Photoelectrochemical lithium extraction. Nano Energy *115*, 108683. https://doi.org/10.1016/j.nanoen.2023.108683.

19. Li, Z., Li, Z., Huang, H., Yao, Y., Khan, B., Zhu, Y., Huang, K.W., Lai, Z., and He, J.H. (2023). Green lithium: photoelectrochemical extraction. PhotoniX *4*, 23. https://doi.org/10.1186/s43074-023-00100-9.

20. Fu, L., Hu, Y., Lin, X., Wang, Q., Yang, L., Xin, W., Zhou, S., Qian, Y., Kong, X.Y., Jiang, L., and Wen, L. (2023). Engineering Multi-field-coupled Synergistic Ion Transport System Based on the Heterogeneous Nanofluidic Membrane for High-Efficient Lithium Extraction. Nano-Micro Lett. *15*, 130. https://doi.org/10.1007/s40820-023-01106-5.

21. Wei, C., Rao, R.R., Peng, J., Huang, B., Stephens, I.E.L., Risch, M., Xu, Z.J., and Shao-Horn, Y. (2019). Recommended Practices and Benchmark Activity for Hydrogen and Oxygen Electrocatalysis in Water Splitting and Fuel Cells. Adv. Mater. *31*, 1806296. https://doi.org/10.1002/adma.201806296.

22. Mariappan, C.R., Yada, C., Rosciano, F., and Roling, B. (2011). Correlation between micro-structural properties and ionic conductivity of $Li_{1.5}Al_{0.5}Ge_{1.5}(PO_4)_3$ ceramics. J. Power Sources *196*, 6456–6464. https://doi.org/10.1016/j.jpowsour.2011.03.065.

23. Zhang, M., Pan, H., Wang, Y., Yang, J., Dong, H., He, P., and Zhou, H. (2023). Research on Li^+/Na^+ Selectivity of NASICON-Type Solid-State Ion Conductors by First-Principles Calculations. Energy Fuel. *37*, 10663–10672. https://doi.org/10.1021/acs.energyfuels.3c01502.

24. Kumar, A., Fukuda, H., Hatton, T.A., and Lienhard, J.H., V (2019). Lithium Recovery from Oil and Gas Produced Water: A Need for a Growing Energy Industry. ACS Energy Lett. *4*, 1471–1474. https://doi.org/10.1021/acsenergylett.9b00779.

25. Pure Energy Minerals (2020). Pure energy reports analytical results from well CV-9 at Clayton Valley lithium brine project. https://pureenergyminerals.com/pure-energy-reports-analytical-results-from-well-cv-9-at-clayton-valley-lithium-brine-project/.

26. Orocobre, P. (2023). Salar de Olaroz – Olaroz Lithium Facility. https://www.datocms-assets.com/53992/1698636645-olaroz-lithium-facility-ni-43-101-technical-report-feasibility-study_final.pdf.

27. Zhao, Z., Liu, G., Jia, H., and He, L. (2020). Sandwiched liquid-membrane electrodialysis: Lithium selective recovery from salt lake brines with high Mg/Li ratio. J. Membr. Sci. *596*, 117685. https://doi.org/10.1016/j.memsci.2019.117685.

28. Badruzzaman, M., Oppenheimer, J., Adham, S., and Kumar, M. (2009). Innovative beneficial reuse of reverse osmosis concentrate using bipolar membrane electrodialysis and electrochlorination processes. J. Membr. Sci. *326*, 392–399. https://doi.org/10.1016/j.memsci.2008.10.018.

29. Bunani, S., Yoshizuka, K., Nishihama, S., Arda, M., and Kabay, N. (2017). Application of bipolar membrane electrodialysis (BMED) for simultaneous separation and recovery of boron and lithium from aqueous solutions. Desalination *424*, 37–44. https://doi.org/10.1016/j.desal.2017.09.029.

30. Afifah, D.N., Ariyanto, T., Supranto, S., and Prasetyo, I. (2018). Separation of Lithium Ion from Lithium-Cobalt Mixture using Electrodialysis Monovalent Selective Ion Exchange Membrane. Eng. J.-Thail. *22*, 165–179. https://doi.org/10.4186/ej.2018.22.3.165.

31. Ji, Z.Y., Chen, Q.B., Yuan, J.S., Liu, J., Zhao, Y.Y., and Feng, W.X. (2017). Preliminary study on recovering lithium from high Mg^{2+}/Li^+ ratio brines by electrodialysis. Sep. Purif. Technol. *172*, 168–177. https://doi.org/10.1016/j.seppur.2016.08.006.

32. Hwang, C.W., Jeong, M.H., Kim, Y.J., Son, W.K., Kang, K.S., Lee, C.S., and Hwang, T.S. (2016). Process design for lithium recovery using bipolar membrane electrodialysis system. Sep. Purif. Technol. *166*, 34–40. https://doi.org/10.1016/j.seppur.2016.03.013.

33. Guo, Z.Y., Ji, Z.Y., Chen, Q.B., Liu, J., Zhao, Y.Y., Li, F., Liu, Z.Y., and Yuan, J.S. (2018). Prefractionation of LiCl from concentrated seawater/salt lake brines by electrodialysis with monovalent selective ion exchange membranes. J. Clean. Prod. *193*, 338–350. https://doi.org/10.1016/j.jclepro.2018.05.077.

34. Li, Y., Shi, S., Cao, H., Wu, X., Zhao, Z., and Wang, L. (2016). Bipolar membrane electrodialysis for generation of hydrochloric acid and ammonia from simulated ammonium chloride wastewater. Water Res. *89*, 201–209. https://doi.org/10.1016/j.watres.2015.11.038.

35. Mickley and Associates (2006). Membrane Concentrate Disposal: Practices and Regulation (US Department of the Interior, Bureau of Reclamation, Technical Service Center, Water Treatment Engineering and Research Group).

36. Jaganmohan, M. (2024). Average lithium carbonate price in 2022. https://www.statista.com/statistics/606350/battery-grade-lithium-carbonate-price/.

37. Galama, A., Post, J., Cohen Stuart, M., and Biesheuvel, P. (2013). Validity of the Boltzmann equation to describe Donnan equilibrium at the membrane–solution interface. J. Membr. Sci. *442*, 131–139. https://doi.org/10.1016/j.memsci.2013.04.022.

38. Jiang, C., Wang, Y., Wang, Q., Feng, H., and Xu, T. (2014). Production of Lithium Hydroxide from Lake Brines through Electro–Electrodialysis with Bipolar Membranes (EEDBM). Ind. Eng. Chem. Res. *53*, 6103–6112. https://doi.org/10.1021/ie404334s.